Astronomy
&
Astrophysics

Anomaly distribution of quasar magnitudes: a test of lensing by a hypothetic supergiant molecular cloud in the Galactic halo

E. Giraud

Laboratoire Univers et Particules, UMR5299 CNRS-In2p3/Montpellier University, 34095 Montpellier, France
Laboratoire d'Astrophysique de Marseille, UMR7236 CNRS-INSU/Aix-Marseille University, 13388 Marseille, France
e-mail: edmond.giraud@lpta.in2p3.fr

ABSTRACT

Context. An anomaly in the distribution of quasar magnitudes based on the Sloan Digital Sky survey, was reported by Longo. The angular size of this quasar anomaly is on the order of $\pm 15°$ on the sky. A smooth low surface brightness structure detected in γ-rays and at 408 MHz, coincides with the sky location and extent of the anomaly, and is close to the northern component of a pair of γ-ray bubbles discovered in the *Fermi Gamma-ray Space Telescope* survey. Molecular clouds are thought to be illuminated by cosmic rays. Molecular gas in the Galaxy, in the form of cold H_2, may be a significant component of dark matter as suggested by Pfenniger et al.
Aims. I test the hypothesis that the magnitude anomaly in the quasar distribution, is due to lensing by a hypothetical supergiant molecular cloud (SGMC) either in or falling into the Galactic halo.
Methods. A series of grid lens models are built by assuming that a SGMC is a fractal structure constructed with clumps of $10^{-3}\ M_\odot$, 10 AU in size, and considering various fractal dimensions. Local amplifications are computed by using the single-plane approximation.
Results. A complex network of caustics due to the clumpy structure is present. Our best single plane lens model capable of explaining Longo's effect, *at least in sparse regions*, requires a mass $(1.5-4.1) \times 10^{10}\ M_\odot$ within $8.7 \times 8.7 \times (5-8.6)$ kpc^3 at a lens plane distance of 20 kpc, and is constructed from a molecular-cloud building-block of $5 \times 10^5\ M_\odot$ within a scale of 30 pc expanded by fractal scaling with dimension $D = 1.8-2$ out to $5-8.6$ kpc for the SGMC. The mass budget depends on the cloud depth and on the fractal dimension.
Conclusions. If such a SGMC were found to exist, it may provide at least part of a lensing explanation for the luminous anomaly discovered in quasars and red galaxies.

Key words. gravitational lensing: micro – ISM: clouds – Galaxy: halo – quasars: general – dark matter – gamma rays: ISM

1. Introduction

An anomaly in the distribution of quasar magnitudes based on the Sloan Digital Sky Survey (SDSS), was reported by Longo (2012). The effect, which is an enhancement on the order of 0.2 mag, is statistically extremely significant in amplitude, and rather well-defined in angular size. A first hint of this anomaly was visible in quasar data as early as three decades ago (Giraud & Vigier 1983). Abate & Feldman (2012) reported a similar enhancement in the distribution of SDSS luminous red galaxies. Because the luminous anomaly does not seem to depend on color, a possible physical explanation is gravitational lensing. Nevertheless, if the lens is at a cosmological distance, its huge angular extent translates into a lens radius ~350 Mpc, and its critical surface density implies a total mass on the order of $10^{21}\ M_\odot$, which is barely consistent with ΛCDM cosmology. A major reason to test a lensing hypothesis with a lens at a *short* distance from the observer, possibly in the Galactic halo, is the large angular extent of the effect combined with its low amplitude.

Two large γ-ray low-surface-brightness bubbles, extending 50° above and below the Galactic center were discovered by Su et al. (2010) in the *Fermi* Gamma-ray Space Telescope survey. These bubbles are spatially correlated with a microwave excess in WMAP. Both the *Fermi* bubbles and the WMAP haze can be explained in terms of synchrotron and inverse-Compton radiation from a hard electron population (Dobler et al. 2010). In addition to the bubbles in the *Fermi* map, there is a single large

faint structure east of the northern bubble ($l \approx -60°$, $b \approx 60°$), which coincides with the quasar anomaly. Any molecular cloud, if present in this faint structure, would be illuminated by cosmic rays escaping from the northern bubble. Cosmic ray/nucleon interactions in molecular clouds were discussed by e.g. Aharonian & Atoyan (1996), de Paolis et al. (1999), Kalberla et al. (1999), Sciama (1999), and Shchekinov (2000). The spectra of γ-rays arising from molecular clouds illuminated by cosmic rays were re-examined by Ohira et al. (2011). The angular extension of the γ-ray structure is consistent with that of the quasar luminosity anomaly. We make the working hypothesis that γ-rays coming from the faint structure trace a supergiant cold molecular cloud (SGMC) in the Galactic halo.

A large fraction of molecular gas in the Galaxy is in the form of cold H_2, and may be a significant component of dark matter (Pfenniger et al. 1994). The variation in the universal rotation curves (Persic et al. 1996) with mass in spiral galaxies may be interpreted as an increasing fraction of baryonic dark matter with decreasing mass of galaxies (Giraud 2000a,b, 2001). The fractal structures of molecular gas clouds, their formation, thermodynamics, and stability have been intensively studied (Scalo 1985; Henriksen 1991; Falgarone et al. 1991; Walker & Wardle 1998; Irwin et al. 2000). The existence of small dark clumps of gas in the Galaxy has been invoked to explain extreme scattering events of quasars (Fielder et al. 1987, 1994). The duration of these events suggests that the sizes and masses of individual cloudlets are on the order of 10 AU and $10^{-3}\ M_\odot$. These values of mass

Table 1. Main parameters for lens mass models.

Model	$\triangle$ (AU)	f	Σ ($M_\odot\,\mathrm{pc}^{-2}$)	$\langle\mu\rangle$	ρ ($M_\odot\,\mathrm{pc}^{-3}$)	M_1 ($M_\odot$)
A	10 000	1	8×10^3	1.18	8	8×10^9
B	9856	1	9×10^3	1.21	9	9×10^9
C	7590	1	2×10^4	1.53	20	2×10^{10}
D	4760	1	8×10^4	25	80	8×10^{10}
E	4760	0.048	8×10^4	25, 1.2	80	3.8×10^9
F	4575	0.012	9×10^4	100, 1.2	90	10^9

Notes. The columns indicate respectively: model identification, mean separation $\triangle$ between clumps, 2 D filling factor f, average surface density in filled area Σ for a 1 kpc depth, average amplification $\langle\mu\rangle$, mass density ρ per pc^3, mass M_1 of a SGMC of 1 kpc^3. In models E & F, the density is given for the dense regions, and the magnification is given for both the dense regions and on average.

and size are also consistent with the searches for lensing toward the LMC (Draine 1998). Cloudlets can survive if the number of collisions is sufficiently small, and their stability is best explained if they are self-gravitating (Combes 2000). Concerning lensing, the average surface density of a SGMC would be subcritical, but the chaotic structure of the matter distribution may lead to a network of caustics with high local magnification.

In the present Letter, I test the hypothesis that the magnitude anomaly in the quasar distribution can be explained in terms of lensing by a hypothetic SGMC in the Galactic halo.

2. Micro lensing and cloud lens models

2.1. Introduction

The lensing of distant galaxies and quasars shears and magnifies their images. There are extensive reviews and books written on lensing including Schneider et al. (1992), Mellier (1999), Schneider (2005), and public algorithms. Fundamental theory, ray-tracing algorithms (Valle & White 2003), and observational techniques have been developed for two to three decades to infer cluster mass distributions (Gladders et al. 2002), large-scale structures, and cosmological models (Soucail et al. 2004; Wambsganss et al. 1997, 2004; Sand et al. 2005).

Systematic studies of micro-lensing were initiated in the early 90s, by Wambsganss (1990), who developed ray-shooting simulations to show the magnification pattern of star fields. In the present paper, we use mainly the software LensTool (Jullo et al. 2007), which includes strong and weak lens regimes.

The change in direction of a light ray can be written

$$\mathrm{d}\boldsymbol{a} = -2\,\mathrm{grad}\,\phi\,\mathrm{d}\chi,$$

where d$\boldsymbol{a}$ is the bend angle, grad is the spatial gradient perpendicular to the light path, ϕ is the gravitational potential, and χ is the radial co-moving coordinate. The distortion can be entirely described by the linearized lens mapping through the Jacobi matrix $\mathbf{A}$ of transform. This matrix is normally expressed with three terms depending on the derivatives of the lensing potential: the convergence κ, the amplitude of the shear γ, and the rotation ω. The convergence changes the radius of a circular source, the shear changes its ellipticity, and the rotation angle is the phase of the shear. Rotation occurs in the case of multiple lens planes.

The convergence $\kappa = \frac{1}{2}(\partial_1^2 + \partial_2^2)\,\phi$ at location θ is related to the projected surface density $\Sigma(\theta)$ at that location by $\kappa(\theta) = \Sigma(\theta)/\Sigma_{\mathrm{crit}}$ in which the critical surface density Σ_{crit} is given by

$$\Sigma_{\mathrm{crit}} = \frac{c^2}{4\pi G}\frac{D_\mathrm{s}}{D_\mathrm{l}D_\mathrm{ls}},$$

where D_s, D_l, and D_ls are, respectively, the distances from observer to source, from observer to lens, and from lens to source. The shear components are $\gamma_1 = \frac{1}{2}(\partial_1^2 - \partial_2^2)\,\phi$ and $\gamma_2 = \partial_1\partial_2\,\phi$.

The present Letter focusses on micro-lensing by numerous clumps; the convergence and the shear of any underlying smooth component is ignored.

2.2. Preliminary test lens models

The critical surface density of a smooth lens located in the Galactic halo on distant objects such that $D_\mathrm{s} \approx D_\mathrm{ls}$ and assuming $D_\mathrm{l} = 15$ kpc is found to be $10^5\ M_\odot\,\mathrm{pc}^{-2}$, which leads to a mass of $10^{14}\ M_\odot$ for a kpc scale SGMC, hence a 3D filling factor on the order of 10^{-4} is required to fit in the halo. A series of grid models of a kpc-size depth, with individual clumps of mass $10^{-3}\ M_\odot$, 10 AU in diameter, were developed with various filling factors.

The cloud models were constructed as follows: an initial FITS frame of 4000×4000 pixels with zero intensity including grids on the order of $10-100$ pixels with a common value of one was created, so that typical separations on the order of $\triangle \sim 10\,000$ AU were reached by assuming a physical pixel size of 10 AU. A series of layers were obtained by randomly shifting the coordinates of the initial frame, which we co-added. We repeated this shift-and-add procedure on the first co-added layer to get a second generation, and repeated again the process up to the required number of generations.

Lens mass models were obtained by multiplying the final frames by the mass of an individual clump, assuming that luminous pixels are *point masses*. Lens simulations with LensTool were done for small sections of the final frames.

Three cases were first considered: $\kappa = 0.2$, to enable us to compare our simulations with those in the literature, $\kappa = 0.09$ because the theoretical mean amplification calculated from $\langle\mu\rangle = 1/|(1 - \kappa)^2 - \gamma^2|$ and assuming $\gamma = 0$ is that of Longo's effect $\langle\mu\rangle = 1.2$, and $\kappa = 0.8$ and 0.9 to explore cases with high magnification and dense caustics. In the case $\kappa = 0.2$, individual caustics can be identified, there are perturbations of single-point caustics by other point masses giving complicated caustic structures comparable with those shown in Wambganss (1990). For $\kappa = 0.09$, the magnification pattern differs from the case $\kappa = 0.2$: individual caustics can be identified but there is almost no perturbation of single clump caustics by other clumps presumably because the density is low. For $\kappa = 0.8$, the magnification pattern shows that there is a high clustering of caustics, with huge amplification at some locations. Model parameters are in Table 1.

Reducing the size of the grid cells quickly boosts the amplification. All these kpc^3 test models however are by far too massive to be used as elementary modules of a SGMC on the order of 500 kpc^3. Low filling factors are necessary.

Table 2. Main parameters for fractal lens mass models.

Model	D_l	D	$M_{min}(M_\odot)$	L_{min}(pc)	L(kpc)	N	Σ $(M_\odot\,pc^{-2})$	μ	M_5 $(M_\odot)$	M_{Tot} $(M_\odot)$
G	16	1.64	5×10^5	30	5	4500	8.9×10^3	1.03	2.2×10^9	–
H	16	2	5×10^5	30	5	27 750	1.7×10^4	1.12	1.4×10^{10}	–
I	20	1.8	5×10^5	30	5	10 106	1.2×10^4	1.12	5×10^9	–
J	20	2	5×10^5	30	8.6	82 095*	2.4×10^4	1.15	–	4.1×10^{10}

Notes. The columns indicate respectively: model identification, lens plane distance D_l, fractal dimension D, mass of building block M_{min}, scale of building block L_{min}, depth of SGMC L, number N of building blocks within 125 kpc^3 (*within 636 kpc^3), maximum integrated surface density Σ, median magnification μ, mass M_5 of a SGMC within 125 kpc^3. total mass M_{Tot} within 636 kpc^3.

2.3. Constrained lens models

Our lens mass-models must have densities lower than the limit of molecular cloud cores: if we assume a maximum mass $\sim 10\ M_\odot$ within a scale length of $L \sim 0.1$ pc above which molecular clouds would collapse (Kayama et al. 1996), and extrapolate this density using the Larson (1981) scaling law $\rho \propto L^{-1.1}$, one gets an upper limit density $\sim 350\ M_\odot\,pc^{-3}$ for a scale length of ~ 100 pc. While our densities satisfy this criterium, a molecular cloud in equilibrium with scale 30 pc, close to our building block, would have a typical mass $\sim 5 \times 10^5\ M_\odot$ (Solomon et al. 1987), and a density 18.5 $M_\odot\,pc^{-3}$, which is significantly below that of models D, E, and F.

A solution may come from a fractal structure of molecular clouds where rather small cells satisfying the equilibrium condition, are separated by less dense regions, and assembled in giant molecular clouds up to a SGMC, as proposed by Pfenniger & Combes (1994, hereafter PC) for cold dark H_2 clouds. A cloud cell of $5 \times 10^5\ M_\odot$ for a scale 30 pc is used as a building block for fractal SGMC models below.

If masses obey a fractal scaling relation with dimension D from mass M_{min} to M_{max} and scale L_{min} to L_{max}, one may write

$$\frac{M}{M_{min}} = \left(\frac{L}{L_{min}}\right)^D$$

up to L_{max}. The mass at level l consists in a number of clumps N at level $l-1$ related to the scale by the relation: $L_{l-1}/L_l = N^{-1/D}$. Clouds can survive if the number of collisions is sufficiently small, which according to PC and Irwin et al. (2000) requires $1 \leq D \leq 2$. If $D \geq 2.33$, internal and external collisions are too numerous to maintaini a fragmented cloud. Two cloud models with two fractal dimensions are considered first: the case $D = 1.64$, which was suggested in the original PC paper, and the upper value of $D = 2$.

Extrapolating from $L_{min} = 30$ pc, and $M_{min} = 5 \times 10^5\ M_\odot$ to $L_{max} = 5$ kpc, and assuming a fractal dimension $D = 1.64$, one gets a total mass $M_{max} = 2.2 \times 10^9\ M_\odot$ within 125 kpc^3, and $N \sim 4500$ cloud cells, i.e. ~ 16 building blocks on each axis. The surface density integrated over a column $L_{max} = 5$ kpc of 16 blocks is $\Sigma = 8.9 \times 10^3\ M_\odot\,pc^{-2}$, which is its maximum value. Parameters of this model are given in Table 2 (model G). The median magnification derived from the probability $p(n)$ of a light ray crossing $0 \leq n \leq 16$ cloud blocks, is found to be $\sum \mu(n)p(n) = 1.03$, so half the surface provides a magnification between 1.20 and 1.03, which is insufficient to explain Longo's effect.

The case $D = 2$ has different properties (model H). Being more populated than for $D = 1.67$, the densities are higher, the median amplification is $\mu = 1.12$, and 25% of the surface has $1.18 \leq \mu \leq 1.48$. Regions with $\mu \geq 1.18$ do show networks of caustics and non-Gaussian amplification distributions. Model H appears to be at the limit of explaining Longo's effect with a

mass of $4.1 \times 10^{10}\ M_\odot$ within 28°. Explaining Longo's effect with greater confidence would require a larger distance and depth of the lens.

2.4. Distance to the lens plane and depth of the lens

Locating the lens plane at an observer distance $D_l = 20$ kpc rather than 16 kpc, reduces the critical surface density by 25% to $\Sigma_{crit} = 7.5 \times 10^4\ M_\odot\,pc^{-2}$ for infinitely distant objects. For this critical surface density, the same amplifications as in model H, are obtained for a cloud with $D = 1.80$, a mass $5 \times 10^9\ M_\odot$ within 125 kpc^3, and a total mass $1.5 \times 10^{10}\ M_\odot$ for a SGMC that is 5 kpc in depth and extends over 8.7×8.7 kpc^2 (model I).

Increasing the depth to 8.6 kpc and using a dimension $D = 2$, we obtain model J, which provides a median amplification of $\mu = 1.15$, with 14% of the surface being amplified by more than 1.5. The total mass within $8.6 \times 8.6 \times 8.6$ kpc^3 is $4.1 \times 10^{10}\ M_\odot$.

A single-plane lens model was assumed. If the cloud were spread over a large distance in depth, the distant part of the lens would be more efficient than the nearby one. There would be a distance shift between the illuminated area and the average lens plane.

2.5. Shear

The shear was not considered in our models. This is because the shear is a term resulting from the mass outside the light beam, such as a smooth galactic component in a star field. In our case however, cloud blocks are mass concentrations that may induce a shear component. Shear is found to be significant in grid sections of average amplification $\mu = 1.1$ and above, but there is a large spread. Assuming $\gamma = \kappa$, the amplification would slightly change, so the same amplifications as for model with $D = 2$ would be obtained with $D = 1.93$.

To summarize, the local lensing hypothesis requires a lens with linear size twice that of the LMC, and a mass a few times that of this satellite. A major difference between the SGMC and the LMC in terms of lensing, is that the SGMC is fully transparent without dust, and is populated by billions of objects with a mass similar to Jupiter.

2.6. Detectability

The SGMC coincides with a $\sim 18-28$ K region in the 408 MHz survey from Haslam et al. (1982), as shown in Fig. 1 (also visible at 1.4 GHz). The coincidence between the Fermi map and that at 408 MHz can be understood if both originate from the same cosmic-ray populations (Su et al. 2010). This may occur at the front of the SGMC or in an ISM feature in the foreground.

Emission from CO is commonly used to trace H_2. With a high column density in H_2, owing to the large depth of the cloud, $3-4 \times 10^{24}$ cm^{-2}, one may expect a rather high value of integrated CO. The conversion factor $X_{CO} = N_{H_2}/W_{CO}$, however,
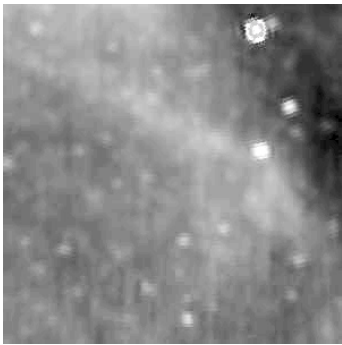
Fig. 1. Temperature map at 408 MHz of the field $30° \times 30°$ centered at RA = 195°, Dec = 0°, from Haslam et al. (1982).

depends strongly on the cloud optical thickness. Glover & Mac Low (2011) obtained a sharp fall-off in $W_{CO} \propto A_V^{-3.5}$ with visual extinction. From the empirical relation $X_{CO} = 2 \times 10^{20} (A_V/3.5)^{-3.5}$ cm^{-2} K^{-1} km^{-1} s, we obtain $W_{CO} < 0.1$ K km s^{-1} for $A_V < 0.1$.

A region of shock in front of the SGMC might produce HI. The HI column density from Dickey & Lockman (1990) in our $30° \times 30°$ field has in fact a low value of $1.5-3 \times 10^{20}$ cm^{-2}.

2.7. Dynamical constraints and long time evolution

The internal kinematics and stability conditions of the SGMC must be similar to those of the LMC, which indicates that it is dynamically stable, despite experiencing internal velocities as high as 220 km s^{-1}. Because the SGMC does not show evidence of HI, Hα, dust and star formation, it should be entering the Galaxy halo for the first time, while being at the location of an encounter. Owing to the findings for the LMC, a SGMC is able to cross the Galactic plane without being disrupted, although it does produce long tails. If the SGMC is falling toward the Galactic plane, it will experience tidal forces, ram pressure, UV and shock heating. Star formation may be triggered while crossing the Galactic plane, and the SGMC may become an irregular dwarf satellite.

2.8. H$_2$ clumps and WIMPS

H$_2$ clumps are extremely dense compared to WIMP clumps of the same mass, as predicted by N-body simulations (Diemand et al. 2005; Springel et al. 2008). A WIMP clump seeded by an H$_2$ clump of the same mass $M = 10^{-3}$ $M_\odot$ will experience a first infall during which its density will increase by 10^6 in ~ 1 Myr. If WIMPS are low-mass neutralinos of $m_\chi \sim 10$ GeV that have an annihilation cross-section $\sigma_{V=0} = 10^{-26}$ cm^3 s^{-1} (Cerdeno et al. 2012), those concentrated in a clump will experience significant annihilation, leading to a mass transform 1.4×10^{-7} $M_\odot$ Myr^{-1} mainly into p, $p-$ and γ. The cumulated mass-loss of those neutralinos is 50% in ~ 6 Gyr, thus an upper limit of $\sim 50\%$ of the clump mass may remain in WIMPs within 10 AU over cosmological ages.

3. Conclusion

A luminosity excess of 0.2 mag was discovered in an SSDS survey of quasars. This effect, which has a huge spatial extent on the order of 30°, is extremely well-determined statistically, and coincides with a large and diffuse region detected in γ-ays by the *Fermi* Gamma-ray Space Telescope.

We have made the working hypothesis that the detected γ luminosity traces a SGMC illuminated by cosmic rays, at least at

its front-end, and test the hypothesis of whether such a cloud would be capable of explaining the quasar luminosity excess by micro-lensing.

Cloud models are built by using compact clumps of mass 10^{-3} $M_\odot$, 10 AU in size, as implied by extreme scattering events on quasars, typical molecular cloud building blocks of mass 5×10^5 $M_\odot$ for a scale of 30 pc, and a fractal structure of the SGMC with dimension $1.64 \leq D \leq 2$ up to a scale of $5-8.6$ kpc.

A SGMC located at a distance of $D_l = 20$ kpc from the observer, that is 8.6 kpc in depth and has a fractal dimension $D = 2$ appears to be capable of explaining Longo's effect with a mass of 4.1×10^{10} $M_\odot$, which is four times that of the LMC.

References

Abate, A., & Feldman, H. 2012, MNRAS, 419, 3482
Aharonian, F. A., & Atoyan, A. 1996, A&A, 309, 917
Cerdeno, D. G., Delahaye, T., & Lavalle, J. 2012, Nucl. Phys. B, 854, 738
Combes, F. 2001, in Molecular hydrogen in space, eds. F. Combes, & G. Pineau des Forêts (Cambridge University Press), 275
de Paolis, F., Ingrosso, G., Jetzer, P., & Roncadelli, M. 1999, ApJ, 510, L103
Dickey, J. M., & Lockam, F. J. 1990, ARA&A, 28, 215
Diemand, J., Moore, B., & Stadel, J. 2005, Nature, 433, 389
Dobler, G., Finkbeiner, D. P., Cholis, I., Slatyer, T. R., & Weiner, N. 2010, ApJ, 717, 825
Draine, B. T. 1998, ApJ, 509, 41
Falgarone, E., Phillips, T. G., & Walker, C. K. 1991, ApJ, 378, 186
Fiedler, R. L., Dennison, B., Johnston, K. J., & Hewish, A. 1987, Nature, 326, 675
Fiedler, R., Dennison, B., Johnston, K. J., Waltman, E. B., & Simon, R. S. 1994, ApJ, 430, 581
Giraud, E. 2000a, ApJ, 544, L41
Giraud, E. 2000b, ApJ, 539, 115
Giraud, E. 2001, ApJ, 558, L23
Giraud, E., & Vigier, J.-P. 1983, in Quasars and Gravitational Lenses, Liège International Astrophysical Colloquium LIACo, 24, 380
Gladders, M. D., Yee, H. K. C., & Ellingson, E. 2002, AJ, 123, 1
Glover, S. C. O., & Mac Low, M.-M. 2011, MNRAS, 412, 337
Haslam, C. G. T., Salter, C. J., Stoffel, H., & Wilson, W. E. 1982, A&AS, 47, 1
Henriksen, R. N. 1991, ApJ, 377, 500
Irwin, J. A., Widraw, L. M., & English, J. 2000, ApJ, 529, 77
Jullo, E., Kneib, J.-P., Limousin, M., et al. 2007, New J. Phys., 9, 447
Kalberla, P. M. W., Shchekinov, Y. A., & Dettmar, R.-J. 1999, A&A, 350, L9
Kamaya, H. 1996, ApJ, 466, L99
Longo, M. J. 2012 [arXiv:1202.4433]
Mellier, Y. 1999, ARA&A, 37, 127
Ohira, Y., Murase, K., & Yamazaki, R. 2011, MNRAS, 410, 1577
Persic, M., Salucci, P., & Stel, F. 1996, MNRAS, 281, 27
Pfenniger, D., & Combes, F. 1994, A&A, 285, 94
Pfenniger, D., Combes, F., & Martinet, L. 1994, A&A, 285, 79
Sand, D. J., Treu, T., Ellis, R. S., & Smith, G. P. 2005, ApJ, 627, 32
Sciama, D. W. 2000a, MNRAS, 319, 1001
Sciama, D. W. 2000b, MNRAS, 312, 33
Scalo, J. M. 1985, in Protostars & Planets II, eds. D. C. Black, & M. S. Matthews (Tucson: Univ. Arizona Press), 201
Schneider, P. 2005, in Gravitational Lensing: Strong, Weak & Micro, eds. G. Meylan, P. Jetzer, & P. North (Berlin: Springer-Verlag), 273
Schneider, P., Ehlers, J., & Falco 1992, Gravitational Lenses (Berlin: Springer-Verlag)
Shchekinov, Y. 2000, Astron. Rep., 44, 65
Solomon, P. M., Rivolo, A. R., Barrett, J., & Yahil, A. 1987, ApJ, 319, 730
Springel, V., White, S. D. M., Frenk, C. S., et al. 2008, Nature, 456, 73
Soucail, G., Kneib, J.-P., & Golse, G. 2004, A&A, 417, L33
Su, M., Slatyer, T. R., & Finkbeiner, D. P. 2010, ApJ, 724, 1044
Vale, C., & White, M. 2003, ApJ, 592, 69
Walker, M., & Wardle, M. 1998, ApJ, 498, L125
Wambsganss, J. 1990, Gravitational Microlensing, Max Planck report 550, MPA Garching
Wambsganss, J., Cen, R., Xu, G., & Ostriker, J. P. 1997, ApJ, 475, L81
Wambsganss, J., Bode, P., & Ostriker, J. P. 2004, ApJ, 606, L93